AGU ADVANCING EARTH AND SPACE SCIENCES

Geophysical Research Letters®

Key Points:

- Observed data shows tropical cyclones contribute 8%–17% of global wind power on near-inertial oscillations
- Tropical cyclones could contribute up to 90% of wind power on near-inertial oscillations in their prone regions
- Accounting for tropical cyclones is essential when estimating wind power on near-inertial oscillations

Tropical Cyclones Related Wind Power on Oceanic Near-Inertial Oscillations

Sheng Lin[1], Yuntao Wang[1] , Wen-Zhou Zhang[2] , Qin-Biao Ni[3] , and Fei Chai[2]

[1]State Key Laboratory of Satellite Ocean Environment Dynamics, Second Institute of Oceanography, Ministry of Natural Resources, Hangzhou, China, [2]State Key Laboratory of Marine Environmental Science, College of Ocean and Earth Sciences, Xiamen University, Xiamen, China, [3]Southern Marine Science and Engineering Guangdong Laboratory (Zhuhai), Zhuhai, China

Abstract Wind power input to oceanic near-inertial oscillations (NIOs) plays a crucial role in sustaining the global ocean conveyor belt. However, the impact of tropical cyclones (TCs) on wind power input to NIOs, despite being the most vigorous atmospheric dynamics capable of exciting NIOs, is often overlooked in global estimations due to their transient nature and a lack of observations. Utilizing hourly wind and ocean current records, we quantified the wind power on NIOs induced by TCs from 1990 to 2019. Our findings reveal that the wind power on NIOs due to TCs is estimated to be between 0.028 and 0.065 TW, which accounts for a significant proportion, that is, 8%–17%, of that over the globe. This study highlights the importance of incorporating the wind power induced by TCs when estimating the global wind power on NIOs, as its impact is non-negligible. Our findings contribute to a better understanding of the global energy balance by improving the estimation of wind power on NIOs.

Plain Language Summary Wind power input to oceanic near-inertial oscillations (NIOs) is important for sustaining the global ocean conveyor belt. However, the influence of tropical cyclones (TCs) on wind power input to NIOs, despite being the most intense atmospheric dynamics that could easily excite NIOs, is often overlooked in global estimations due to their transient nature and a lack of observations. By analyzing wind and ocean current records from 1990 to 2019, the wind power on NIOs induced by TCs was quantified. We found that wind power on NIOs due to TCs is non-negligible and accounts for a significant portion of that over the globe. This study highlights the importance of considering the wind power induced by TCs when estimating the global wind power on NIOs, which helps to achieve a more accurate estimation of wind power on NIOs, leading to an improved understanding of the global energy balance.

1. Introduction

The global ocean conveyor belt plays a crucial role in shaping the Earth's climate by significantly influencing global ocean heat uptake. To maintain this conveyor belt, a substantial energy flux of approximately 2.1 TW is required for the diapycnal mixing (Munk & Wunsch, 1998) that drives global abyssal stratification (Broecker, 1991). Wind-generated near-inertial oscillations (NIOs), internal tides, and lee waves are considered the major sources of energy that fuel diapycnal mixing (Egbert & Ray, 2001; Jayne & St. Laurent, 2001). Among them, internal tides and lee waves are estimated to account for about 1 and 0.2 TW, respectively. The remaining energy required to fuel diapycnal mixing is attributed to wind-generated NIOs (Alford, 2001).

When the wind stress fluctuates at frequencies comparable to the local inertial frequency, such as during winter storms and tropical cyclones (TCs), NIOs can be easily triggered (Pollard, 1970; Price, 1981; D'Asaro, 1985). The majority of wind power on NIOs is concentrated in the 30°–60° zonal region, primarily due to energetic winter storms (Alford, 2020; Liu et al., 2019). Despite TCs are more effective than winter storms in producing NIOs because of their intensive wind stresses, appropriate size, and translation speed (Price et al., 1994; Yang & Hou, 2014), wind power on NIOs induced by TCs is usually neglected due to the transient nature of TCs. However, considering TCs as the most powerful atmospheric systems, capable of efficiently driving NIOs (D'Asaro et al., 1995; Zhang et al., 2020), they could significantly contribute to the wind power on NIOs (Boos et al., 2004; Chen et al., 2013; Emanuel, 2001). Lob et al. (2021) found that the wind power on NIOs induced by a single TC, which lasted only 19 days, was equivalent to the background wind power on NIOs over a period of 150 days. Numerical models have also demonstrated a prominent local enhancement in the annually averaged

wind power on NIOs along the track of TCs, reaching a maximum of 8 mW/m^2, surpassing the annually averaged wind power induced by winter storms, which reaches a maximum of 5 mW/m^2 (Sun et al., 2021). Furthermore, the surface near-inertial energy flux induced by TCs has been found to be particularly efficient in promoting interior mixing (von Storch & Lüschow, 2023).

Various studies have been conducted to estimate the wind power on NIOs, yielding a range of values from 0.26 to 1.5 TW (Alford, 2003, 2020; Jiang et al., 2005; Rimac et al., 2013; Watanabe & Hibiya, 2002). However, recent studies have suggested that wind power on NIOs may be lower than previously assumed (e.g., Alford, 2020; Liu et al., 2019). Liu et al. (2019) specifically used observational data to estimate wind power on NIOs and found that numerical models tend to overestimate this input. Consequently, the relative contribution of TCs in terms of wind energy input may be more important, which has gained significant attention (e.g., Sun et al., 2021). The worldwide wind power on NIOs is expected to be underestimated by 10%–33%, when the wind power on NIOs induced by TCs is overlooked (Alford et al., 2016; von Storch & Lüschow, 2023).

The wind power on NIOs induced by TCs is estimated to be 0.026–0.07 TW, accounting for 5%–27% of the global wind power on NIOs (Alford et al., 2016; Liu et al., 2008; Nilsson, 1995). The variation in results could be attributed to differences in methodology, wind product, or parameterization used in the models (von Storch & Lüschow, 2023). It is important to note that the estimation of TC-induced wind power on NIOs is challenging due to limited observations. Consequently, models are often employed to calculate the wind power input. However, the choice of different models can significantly impact the results (von Storch & Lüschow, 2023). Liu et al. (2008) also proposed several shortcomings of coupled models in simulating currents, including inaccurately initialized oceanic conditions, the absence of air-sea heat flux, and entrainment parameterization. To avoid the deficiencies of models, further studies based on observational current data are necessary to accurately quantify the contribution of TCs to global wind power on NIOs. However, the scarcity of observations during TCs has hindered a comprehensive quantification of the associated wind power on NIOs induced by TCs.

Based on the velocity profile observed during the passage of TC Gilbert, the TC-induced wind power on NIOs is estimated to be approximately 0.74 TW (Shay & Jacob, 2006). This estimate is one order of magnitude larger than the former estimates, indicating that observations from a single TC may not accurately reflect the global wind power on NIOs induced by TCs. This is because TCs can vary significantly in intensity and translation speed, leading to variations in the ocean response to TCs (e.g., Zhang et al., 2020). Estimates of near-inertial wind power induced by TCs based on worldwide observations are thus necessary to improve the estimation and gain a better understanding of air-sea interactions.

Velocity data sets from drifters have indeed been widely utilized to investigate the sea surface current response to TCs (Chang et al., 2013; Fan et al., 2022; Wang et al., 2022). These data sets can also be applied to estimate the global wind power on NIOs (Liu et al., 2019). Using ocean current records derived from surface drifters and wind vectors from analysis products, the climatological wind power on NIOs over the global ocean is estimated to be 0.3–0.6 TW (Liu et al., 2019). However, TC-induced wind power on NIOs has not been considered in the global estimation (Liu et al., 2019), leading to an underestimation of the overall wind power on NIOs (Sun et al., 2021). To obtain a comprehensive understanding of wind power on NIOs and its global contribution, it is crucial to quantify the values of TC-induced wind power on NIOs.

In this study, ocean current records from drifters are used to estimate the wind power on NIOs induced by TCs. The main objective is to determine the relative contribution of TCs to the wind power on NIOs using observed ocean current records. The structure of the paper is as follows: Section 2 provides a description of the methodology and data used in the study. Section 3 presents and discusses the spatial distribution and relative contributions of TCs to the wind power on NIOs. Finally, Section 4 concludes the paper by summarizing the findings.

2. Data and Methodology

2.1. Surface Drifter Observations

This study uses velocity data tracked by the GPS and Argos system (Elipot et al., 2016) from 1990 to 2019 to estimate the wind power on NIOs induced by TCs. To ensure data quality, we discarded records from single drifters that lasted less than 300 hr, resulting in 159,411,472 sample records (16,373 drifters) being retained. The spatial distribution of samples is shown as the number of records in each 2° by 2° grid (Figure 1a). Most
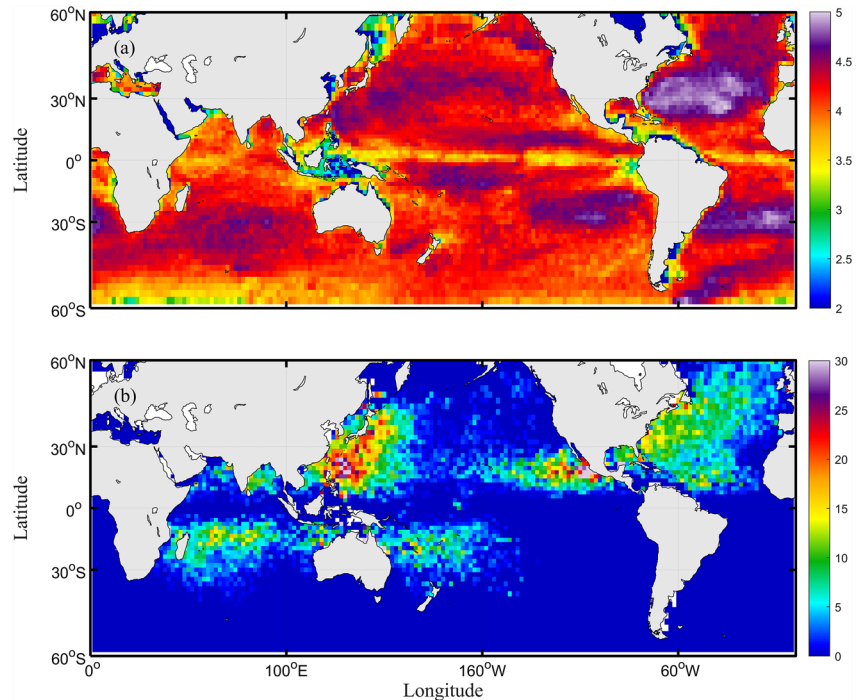
Figure 1. (a) Spatial distribution of drifter samples in $2° \times 2°$ grids represented by the number ($\log_{10}$) of samples. (b) Proportion (in percent) of drifters under the influence of TCs in each grid.

of the boxes between 60°S and 60°N were well-sampled, making it sufficient to compute averaged TC-induced wind power on NIOs. However, the convergence zones, such as the subtropical gyres, are more frequently sampled compared to divergence zones, that is, equatorial, polar, and coastal regions, where fewer records were found.

2.2. Wind Reanalysis Data

To avoid errors caused by temporal interpolation (Jing et al., 2015; Liu et al., 2019), we use hourly ocean surface wind data from the fifth generation European Centre for Medium-Range Weather Forecasts atmospheric reanalysis of the global climate (ERA5) in this study, which has a spatial resolution of 0.25°.

2.3. TCs Best Track Data

We obtain TC data from the best track data set of the International Best Track Archive for Climate Stewardship (IBTrACS), which provides the 6-hourly TC locations and intensity information (Knapp et al., 2010). To ensure consistency with the drifter and wind data, we interpolated the TC data onto hourly time intervals via linear regression. We excluded hourly TC data with a maximum wind speed less than 17 m/s from the study.

2.4. Computation of Near-Inertial Wind Power

Following Liu et al. (2019), we compute the wind power on NIOs (W_I) as follows:

$$W_I = \vec{\tau} \cdot \vec{u_I} \tag{1}$$

where τ is the surface wind stress and u_I is the sea surface near-inertial current. For each drifter observation, we linearly interpolate the simultaneous ERA5 wind onto the drifter position to compute the wind stress. The surface wind stress is evaluated as:

$$\vec{\tau} = \rho_a C_D |\overrightarrow{U_{10}} - \vec{u}| \left(\overrightarrow{U_{10}} - \vec{u} \right) \tag{2}$$
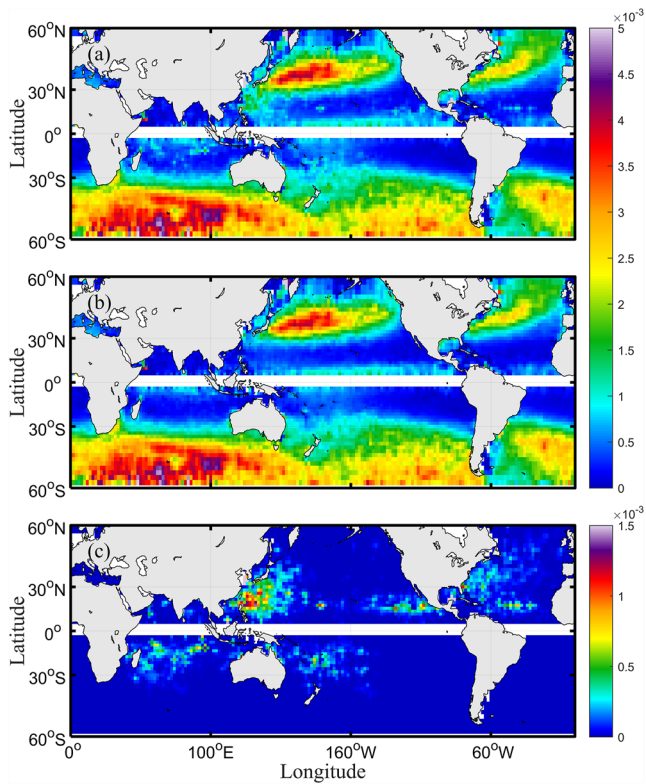
Figure 2. The spatial distribution of wind power (W/m^2) on oceanic NIOs (a) with the influence of TCs and (b) without the influence of TCs computed from the drifters and ERA5 data sets. (c) Contribution of TCs to near-inertial wind power.

where ρ_a is the air density (1.22 kg/m^3), C_D is the drag coefficient based on field experiments in TCs (Powell et al., 2003), U_{10} is the wind vector at 10 m, and u is the ocean current vector.

The near-inertial current is calculated from drifter data using a band-pass filter. The near-inertial band is defined as $0.75f$–$1.25f$, where f is the Coriolis frequency. Following Liu et al. (2019), velocity records tracked by each drifter are broken into half-overlapping 300-hr segments. For each 300-hr segment, the value of f is set as the mean value.

2.5. TCs Induced Near-Inertial Wind Power

The drifters are divided into two groups: drifters under and without the influence of TCs. We use these groups to calculate the TC-related wind power (W_{tc}) and the climatology wind power (W_{climat}). For each hourly TC position and time, the drifters under the influence of TCs must meet the following spatial and temporal criteria: (a) the distance from drifters to TC center should be within 500 km; (b) the drifter sampling time should be within the range from 3 days before the passage of typhoons to 20 days after typhoons (see Text S1 in Supporting Information S1 for the selection of the threshold). A significant number of samples (1,704,590) were used to derive the wind power.

The proportion of drifters under the influence of TCs (P_{tc}) shows peaks in the main TC-prone regions (Figure 1b), reaching more than 20% in the North Pacific. The total wind power on oceanic NIOs in each grid can be estimated as follows:

$$W_{total} = W_{tc} * P_{tc} + W_{climat} * (1 - P_{tc})$$

$$= \overbrace{(W_{tc} - W_{climat}) * P_{tc}}^{W_{contc}} + W_{climat} \tag{3}$$

where $W_{tc}*P_{tc}$ is the contribution of TCs, $W_{climat}*(1-P_{tc})$ is the contribution of climatology, and $(W_{tc}-W_{climat})*P_{tc}$ is the additional contribution of TCs (W_{contc}), representing the value of underestimate when TCs are overlooked ($W_{total}-W_{climat}$).

3. Result and Discussion

3.1. Spatial Variation of Wind Power on Oceanic NIOs

The total wind power (W_{total}) on oceanic NIOs with the influence of TCs reveals significant values in the 30–60° zonal band across both hemispheres (Figure 2a). The global peak value is 4.7 mW/m^2, appearing in the Southern Ocean (Figure 2a). This pattern is in consistent with previous works (Alford, 2020; Liu et al., 2019), due to the passages of winter storms in these regions. The quasi-global integral (60°S to 60°N) of W_{total} is 0.33 TW, which is comparable with Liu et al. (2019), indicating the reliability of the data and methodology employed in this study.

Considering the influence of TCs, the W_{total} in TC-prone region of western North Pacific exhibits values exceeding 1.5 mW/m^2, which is of the same magnitude as the global peak value (Figure 2a). In comparision, the value of W_{climat} in the TC-prone region of western North Pacific is smaller than 0.5 mW/m^2 (Figure 2b). Most of the wind power on NIOs induced by TCs is concentrated in the TC-prone region of North Pacific, especially in the western section in accordance with the TC tracks (Figure 2c). The peak value of W_{contc} in the western North Pacific is 1.5 mW/m^2, which is approximately 10 times larger than the corresponding value of W_{climat} in the same area, accounting for more than 90% of the relative contribution (W_{contr}/W_{total}) of wind work on NIOs. Lob et al. (2021) also found that the energy flux during the storm event is about 7.5 times greater than the background energy flux. Therefore, TCs can be considered as a significant source of wind energy input, especially in TC-prone regions. However, the peak value of W_{contc} was still significantly smaller than the results obtained from CESM simulations

(Sun et al., 2021) and coupled model simulations (Liu et al., 2008). These studies reported peak values exceeding 8 mW/m² in CESM simulations and approximately 3 mW/m² along the TC tracks in the coupled model simulations, respectively. This discrepancy is attributed to the underestimation of wind speeds from ERA5 during TCs, which will be discussed further in Section 3.2.

Prominent enhancement of wind power in the TC-prone region is identified in this study, which is not present in Liu et al. (2019). This difference can be largely attributed to the dissimilarities in the wind products used. Specifically, in the CCMP data set, the intensity of TCs is weaker at 6-hr intervals compared to the 1-hr intervals used in this study. The TCs contribute an additional 0.028 TW (8% of the total) to the wind power on NIOs based on ERA5 reanalysis, larger than that from CCMP (0.018 TW, 5%). Consistently, the enhancement of wind power on NIOs in the TC-prone region is also captured in the wind data set from the Modern-Era Retrospective Analysis for Research and Applications (MERRA) (Rienecker et al., 2011) with a temporal resolution of 1 hr, as indicated in Supporting Information of Liu et al. (2019). It has been documented that the near-inertial band wind stress variation would be partially filtered out when linearly interpolating 6-hourly reanalysis winds into hourly intervals (Jing et al., 2015; Niwa & Hibiya, 1999). This artificial loss of near-inertial wind stress variation leads to a significant underestimation of the wind power on NIOs (Jing et al., 2015). Therefore, it is vital to utilize wind data with high temporal resolution to accurately capture the near-inertial wind power on NIOs.

The quasi-global integral contribution of TCs to the wind power on NIOs (0.028 TW) is comparable to theoretical and model results (Liu et al., 2008; Nilsson, 1995). Because the occurrence of TCs is limited and the TCs induced wind power was generally underestimated, the integrated value of W_{contr} is an order of magnitude smaller than that of W_{climat}; thus, the wind power on NIOs induced by TCs is oftenly overlooked (Liu et al., 2019). This discrepancy is partly due to the fact that the peak value of W_{contc} is only one-third of the global peak induced by wind storms. Moreover, the influence of TCs is considerably less widespread compared to that of wind storms, which typically covers the entire midlatitude zone (Figure 2b). In contrast, the impact of TCs is primarily localized in specific TC-prone zones (Figure 2c).

3.2. Discussion

The precise measurements of sea surface near-inertial currents and surface wind speed is essential for accurate estimation of wind power on NIOs induced by TCs, that is, following Equations 1 and 2. In previous studies, models have been used due to limited observations for conducting direct estimation of TC-induced wind power (e.g., Alford, 2001, 2003; Jiang et al., 2005; Rimac et al., 2013; Watanabe & Hibiya, 2002). The slab model of Pollard and Millard (1970) has been widely used in these studies, but it may lead to an overestimation of global wind work since it fails to consider the role of NIOs in deepening the mixed layer (Alford, 2020; Plueddemann & Farrar, 2006). A model that takes into account mixed layer deepening, such as the Price-Weller-Pinkel model, has shown better agreement with observed estimates of wind power on NIOs (Plueddemann & Farrar, 2006). However, the Price-Weller-Pinkel model also has limitations due to initial oceanic conditions and model parameterization, which can result in an overestimation of global wind work (see Figure 10 of Plueddemann & Farrar, 2006). These model limitations is neatly illustrated by the substantial variability in the results of near-inertial currents obtained from different model results (von Storch & Lüschow, 2023).

In this study, observed sea surface current data from global drifter measurements were utilized, which is expected to provide more accurate information and consequently lead to a more precise estimation of wind power on NIOs induced by TCs. However, it should be noted that there was a limitation in the surface wind speed data used in this study. Figure 3a illustrates the comparisons between the maximum wind speed calculated from ERA5 reanalysis data and the IBTrACS data. It is observed that the maximum wind speed calculated from ERA5 is generally smaller, ranging from 3% to 66%, compared to the IBTrACS data. On average, there is a mean difference of 22% between the two data sets. This discrepancy is consistent with previous studies that have shown that atmospheric reanalysis data tend to underestimate wind speeds during TC events to some extent (e.g., Liu & Sasaki, 2019; Vincent et al., 2012).

To improve the accuracy of the estimated wind field during TCs from ERA5 data, a crude adjustment of wind speeds during TCs was conducted by multiplying the ERA5 values by a factor of the mean difference between ERA5 and the reference data set (ERA5 *1.22 adjustment method). The estimated wind power value obtained using ERA5 *1.22 adjustment method are 0.051 TW, accounting for 14% of the quasi-global integral (60°S to
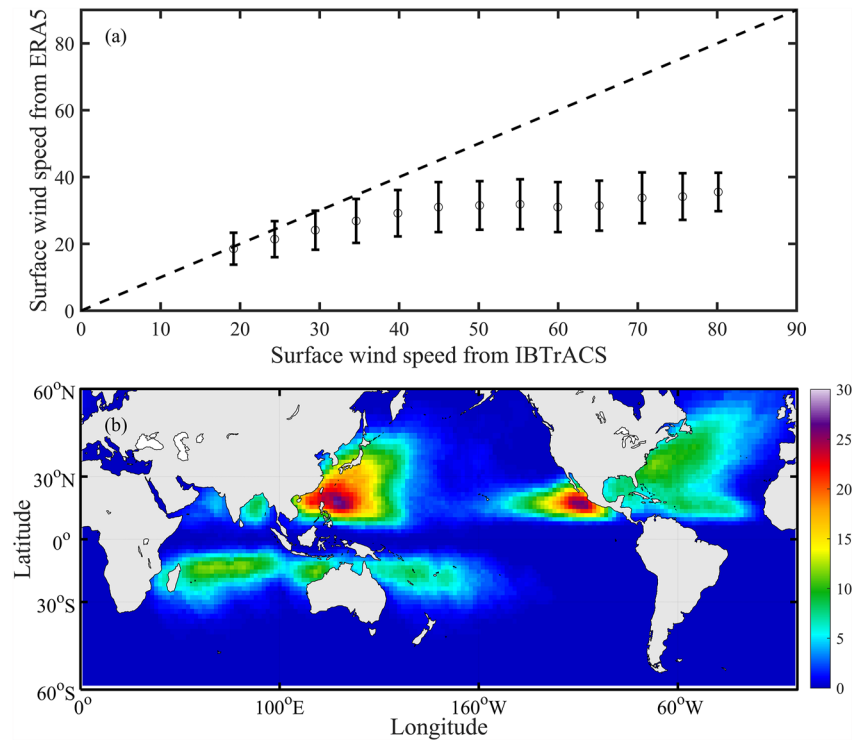
Figure 3. (a) Comparisons of maximum wind speed (m/s) calculated from ERA5 with corresponding results of IBTrACS. (b) Proportion of influencing time of TCs (T_{tc}) calculated from IBTrACS data.

60°N) of W_{total}. To test the reliability of the adjustment method, another two adjustments were conducted based on the idealized vortex spatial structure proposed by Holland (1980) and Willoughby et al. (2006) as described in Supporting Information S1. The estimated wind power values obtained using Holland and Willoughby adjustment methods are 0.054 TW and 0.053 TW, respectively. These estimated wind power values both account for 15% of the quasi-global integral (60°S to 60°N) of W_{total}. The fact that the values derived from different adjustment methods are comparable, indicating that the methods used are reliable.

Besides the underestimate wind speeds, the uncertainty of the estimates can also be influenced by sampling errors. The observed TC-related wind power exhibits a similar pattern to the sampling proportion of drifters (Figure 1b) and the influential time of TCs (Figure 3b). This suggests that the averaged wind power on NIOs induced by TCs is largely dependent on the occurrence of TCs. Former studies identified a striped enhancement of wind power along specific tracks of TCs (Sun et al., 2021; von Storch & Lüschow, 2023). However, these studies were limited to a 1 year simulation period, which may have resulted in a more localized and fragmented representation of TC-induced wind power on NIOs. In contrast, this study benefits from a longer period of 30 years of TC data, allowing for a more comprehensive and objective assessment of TC-induced wind power on NIOs in space. As a result, the estimated TC-related wind power on NIOs in this study exhibits a smoother pattern, capturing the overall spatial distribution of TC-induced wind power on NIOs more accurately.

However, it is important to acknowledge that drifter observations cannot cover the entire time and space, leading to inherent randomness and potential sampling bias under the passage of TCs. The proportion of drifters under the influence of TCs (P_{tc}) may not accurately reflect the actual influencing time of TCs (Figures 1b and 3b). Comparing to T_{tc} (Figure 3b), the P_{tc} (Figure 1b) exhibits evident over-sampling in certain regions such as Arabian Sea, the temperate zone of the western North Pacific, and many nearshore areas. Conversely, some regions, notably the South China Sea, are under-sampling. Considering that the wind power on NIOs induced by TCs is largely dependent on the actual duration of TC influence, it is crucial to address the sampling bias by utilizing T_{tc} instead of P_{tc}. By accounting for the actual duration of TCs, an improved estimation for the contribution of TCs from ERA5*1.22 adjusted data yields a value of 0.061 TW, accounting for 16% of the global near-inertial power input (Figure 4b). Similarly, the values derived from Holland and Willoughby adjusted
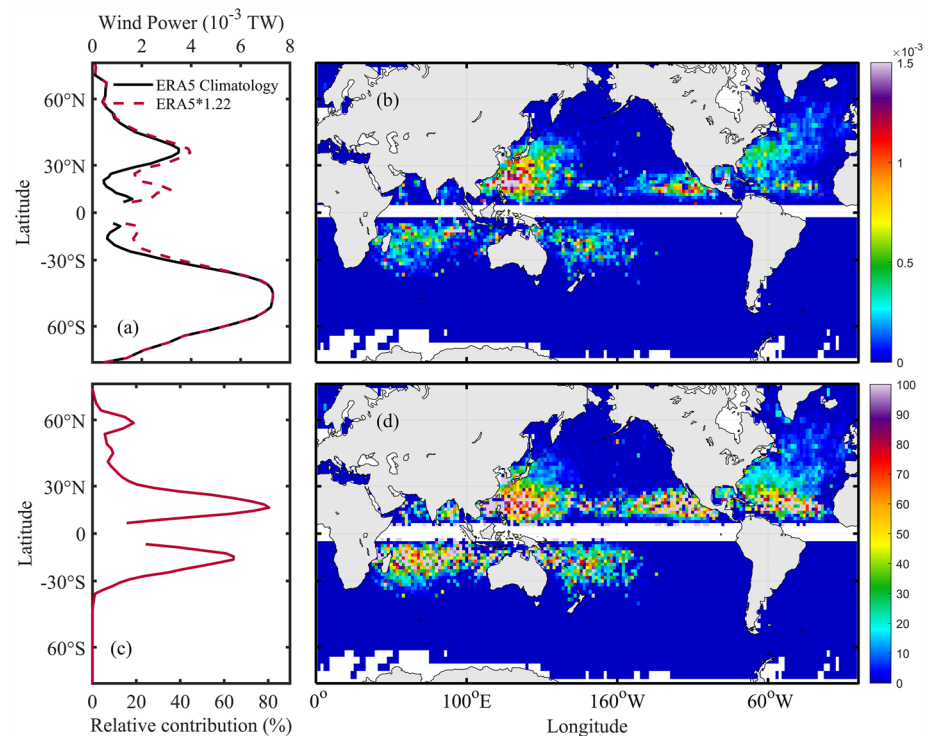
Figure 4. (a) Meridional distribution of zonally integrated wind power on NIOs with (ERA5*1.22, dashed red) and without (Climatology, solid black) the influence of TCs. (b) Additional contribution of TCs to wind power (W/m²) on NIOs (W_{contc}). (c) Meridional distribution of percentage of TC-related wind power on oceanic NIOs (W_{contc}/W_{total}). (d) Percentage of TC-related wind power on oceanic NIOs (W_{contc}/W_{total}). The value of W_{contc} is estimated by considering the influence of the actual duration of TCs, based on the wind fields from ERA5*1.22 adjustment.

data are 0.065 TW and 0.064 TW, respectively, accounting for 17% of the global near-inertial power input (see Supporting Information S1).

The relative contribution of TCs to wind power on NIOs is significant in TC-prone regions, exceeding 40% in majority of these regions (Figure 4d). In fact, TCs can contribute up to 90% of wind power on NIOs in many area, especially in the Northern Hemisphere. Figure 4a illustrates the meridional distribution of the zonally integrated wind power. The maximum value of TC-related wind power on NIOs from ERA5*1.22 adjusted data is 0.0032 TW at 17°N, which is comparable to the maximum climatology wind power on NIOs of 0.0035 TW in the Northern Hemisphere and much greater than the value of 0.0008 TW at 17°N (Figure 4a). Consequently, TCs contribute 80% of the zonal integrated wind power at 17°N (Figure 4c). Notably, TCs could contribute nearly half (49%) of the integrated wind power between 30°S and 30°N (Figure 4c). Indeed, the findings highlight the significant role that TCs play in enhancing wind power and their substantial contribution to zonally integrated wind power in regions with concentrated TC activities, emphasizing their importance in shaping the overall wind dynamics in the global ocean.

4. Conclusion

This study provides an objective estimation of the wind power on NIOs induced by TCs using global observed ocean velocity data. The findings reveal a significant contribution of TCs to the near-inertial power input in the global ocean, accounting for 8%–17% of the total. It is anticipated that this contribution will increase in the future due to the ongoing strengthening of global TCs (Wang et al., 2022). Previous research has already found a 16% increase in near-inertial energy input from TCs between 1984 and 2003 (Liu et al., 2008). Therefore, the energy input from TCs will play an even more crucial role in the future, highlighting the importance of conducting further research to enhance our understanding of the role of TCs in the wind power input on NIOs.

Furthermore, in localized regions prone to TC, TCs play a dominant role in the wind power input on NIOs. This dominance has the potential to influence the local climate system by affecting the mixed layer depth during TC

seasons. Since NIOs contribute to the enhancement of shear at the base of mixed-layer (e.g., Whalen et al., 2020), the wind power on NIOs induced by TCs can significantly deepen the local mixed layer depth in TC-prone regions during TC seasons. These effects, in turn, can have implications for the local climate system. Overall, this study underscores the importance of utilizing accurate wind speed data and emphasizes the need for further research to enhance our understanding of the contribution of TCs to the wind power on NIOs. By gaining a more comprehensive understanding of these dynamics, we can improve climate modeling and prediction, leading to better-informed decision-making processes for managing the impacts of TCs on regional climate systems.

Data Availability Statement

The drifter data were provided by National Oceanic and Atmospheric Administration (Elipot et al., 2022). The tropical cyclone data were obtained from International Best Track Archive for Climate Stewardship (Knapp et al., 2018).

References

Alford, M. H. (2001). Internal swell generation: The spatial distribution of energy flux from the wind to mixed layer near-inertial motions. *Journal of Physical Oceanography*, *31*(8), 2359–2368. https://doi.org/10.1175/1520-0485(2001)031<2359:ISGTSD>2.0.CO;2

Alford, M. H. (2003). Improved global maps and 54-year history of wind-work on ocean inertial motions. *Geophysical Research Letters*, *30*(8), 2002GL016614. https://doi.org/10.1029/2002gl016614

Alford, M. H. (2020). Revisiting near-inertial wind work: Slab models, relative stress, and mixed layer deepening. *Journal of Physical Oceanography*, *50*(11), 3141–3156. https://doi.org/10.1175/JPO-D-20-0105.1

Alford, M. H., MacKinnon, J. A., Simmons, H. L., & Nash, J. D. (2016). Near-inertial internal gravity waves in the ocean. *Annual Review of Marine Science*, *8*(1), 95–123. https://doi.org/10.1146/annurev-marine-010814-015746

Boos, W. R., Scott, J. R., & Emanuel, K. A. (2004). Transient diapycnal mixing and the meridional overturning circulation. *Journal of Physical Oceanography*, *34*(1), 334–341. https://doi.org/10.1175/1520-0485(2004)034<0334:TDMATM>2.0.CO;2

Broecker, W. S. (1991). The great ocean conveyor. *Oceanography*, *4*(2), 79–89. https://doi.org/10.5670/oceanog.1991.07

Chang, Y.-C., Chen, G.-Y., Tseng, R.-S., Centurioni, L. R., & Chu, P. C. (2013). Observed near-surface flows under all tropical cyclone intensity levels using drifters in the northwestern Pacific. *Journal of Geophysical Research: Oceans*, *118*(5), 2367–2377. https://doi.org/10.1002/jgrc.20187

Chen, G., Xue, H., Wang, D., & Xie, Q. (2013). Observed near-inertial kinetic energy in the northwestern South China Sea. *Journal of Geophysical Research: Oceans*, *118*(10), 4965–4977. https://doi.org/10.1002/jgrc.20371

D'Asaro, E. A. (1985). The energy flux from the wind to near-inertial motions in the surface mixed layer. *Journal of Physical Oceanography*, *15*(8), 1043–1059. https://doi.org/10.1175/1520-0485(1985)015<1043:TEFFTW>2.0.CO;2

D'Asaro, E. A., Eriksen, C. C., Levine, M. D., paulson, C. A., Niiler, P., & Van Meurs, P. (1995). Upper-ocean inertial currents forced by a strong storm. Part I: Data and comparisons with linear theory. *Journal of Physical Oceanography*, *25*(11), 2909–2936. https://doi.org/10.1175/1520-0485(1995)025<2909:Uoicfb>2.0.Co;2

Egbert, G. D., & Ray, R. D. (2001). Estimates of M2 tidal energy dissipation from TOPEX/Poseidon altimeter data. *Journal of Geophysical Research*, *106*(C10), 22475–22502. https://doi.org/10.1029/2000JC000699

Elipot, S., Lumpkin, R., Perez, R. C., Lilly, J. M., Early, J. J., & Sykulski, A. M. (2016). A global surface drifter data set at hourly resolution. *Journal of Geophysical Research: Oceans*, *121*(5), 2937–2966. https://doi.org/10.1002/2016JC011716

Elipot, S., Sykulski, A., Lumpkin, R., Centurioni, L., & Pazos, M. (2022). Hourly location, current velocity, and temperature collected from Global Drifter Program drifters world-wide [Dataset]. NOAA National Centers for Environmental Information. https://doi.org/10.25921/x46c-3620

Emanuel, K. (2001). Contribution of tropical cyclones to meridional heat transport by the oceans. *Journal of Geophysical Research*, *106*(D14), 14771–14781. https://doi.org/10.1029/2000jd900641

Fan, S., Zhang, B., Perrie, W., Mouche, A., Liu, G., Li, H., et al. (2022). Observed ocean surface winds and mixed layer currents under tropical cyclones: Asymmetric characteristics. *Journal of Geophysical Research: Oceans*, *127*(2), e2021JC017991. https://doi.org/10.1029/2021jc017991

Holland, G. J. (1980). An analytic model of the wind and pressure profiles in Hurricanes. *Monthly Weather Review*, *108*(8), 1212–1218. https://doi.org/10.1175/1520-0493(1980)108<1212:AAMOTW>2.0.CO;2

Jayne, S. R., & St Laurent, L. C. (2001). Parameterizing tidal dissipation over rough topography. *Geophysical Research Letters*, *28*(5), 811–814. https://doi.org/10.1029/2000GL012044

Jiang, J., Lu, Y. Y., & Perrie, W. (2005). Estimating the energy flux from the wind to ocean inertial motions: The sensitivity to surface wind fields. *Geophysical Research Letters*, *32*(15), L15610. https://doi.org/10.1029/2005GL023289

Jing, Z., Wu, L., & Ma, X. (2015). Improve the simulations of near-inertial internal waves in the ocean general circulation models. *Journal of Atmospheric and Oceanic Technology*, *32*(10), 1960–1970. https://doi.org/10.1175/JTECH-D-15-0046.1

Knapp, K. R., Diamond, H. J., Kossin, J. P., Kruk, M. C., & Schreck, C. J. (2018). International Best Track Archive for Climate Stewardship (IBTrACS) project (version 4) [Dataset]. NOAA National Centers for Environmental Information. https://doi.org/10.25921/82ty-9e16

Knapp, K. R., Kruk, M. C., Levinson, D. H., Diamond, H. J., & Neumann, C. J. (2010). The international best track archive for climate stewardship (IBTrACS): Unifying tropical cyclone best track data. *Bulletin of the American Meteorological Society*, *91*(3), 363–376. https://doi.org/10.1175/2009bams2755.1

Liu, F., & Sasaki, J. (2019). Hybrid methods combining atmospheric reanalysis data and a parametric typhoon model to hindcast storm surges in Tokyo Bay. *Scientific Reports*, *9*(1), 12222. https://doi.org/10.1038/s41598-019-48728-7

Liu, L. L., Wang, W., & Huang, R. X. (2008). The mechanical energy input to the ocean induced by tropical cyclones. *Journal of Physical Oceanography*, *38*(6), 1253–1266. https://doi.org/10.1175/2007jpo3786.1

Liu, Y., Jing, Z., & Wu, L. (2019). Wind power on oceanic near-inertial oscillations in the global ocean estimated from surface drifters. *Geophysical Research Letters*, *46*(5), 2647–2653. https://doi.org/10.1029/2018GL081712

Lob, J., Kohler, J., Walter, M., Mertens, C., & Rhein, M. (2021). Time series of near-inertial gravity wave energy fluxes: The effect of a strong wind event. *Journal of Geophysical Research-Oceans*, *126*(10), e2021JC017472. https://doi.org/10.1029/2021JC017472

Munk, W., & Wunsch, C. (1998). Abyssal recipes II: Energetics of tidal and wind mixing. *Deep Sea Research Part I: Oceanographic Research Papers*, *45*(12), 1977–2010. https://doi.org/10.1016/S0967-0637(98)00070-3

Nilsson, J. (1995). Energy flux from traveling hurricanes to the oceanic internal wave field. *Journal of Physical Oceanography*, *25*(4), 558–573. https://doi.org/10.1175/1520-0485(1995)025<0558:Efftht>2.0.Co;2

Niwa, Y., & Hibiya, T. (1999). Response of the deep ocean internal wave field to traveling midlatitude storms as observed in long-term current measurements. *Journal of Geophysical Research*, *104*(C9), 20857. https://doi.org/10.1029/1999JC900211

Plueddemann, A. J., & Farrar, J. T. (2006). Observations and models of the energy flux from the wind to mixed-layer inertial currents. *Deep Sea Research Part II: Topical Studies in Oceanography*, *53*(1–2), 5–30. https://doi.org/10.1016/j.dsr2.2005.10.017

Pollard, R. T. (1970). On the generation by winds of inertial waves in the ocean. *Deep-Sea Research and Oceanographic Abstracts*, *17*(4), 795–812. https://doi.org/10.1016/0011-7471(70)90042-2

Pollard, R. T., & Millard, R. C. (1970). Comparison between observed and simulated wind-generated inertial oscillations. *Deep-Sea Research and Oceanographic Abstracts*, *17*(4), 813–816. https://doi.org/10.1016/0011-7471(70)90043-4

Powell, M. D., Vickery, P. J., & Reinhold, T. A. (2003). Reduced drag coefficient for high wind speeds in tropical cyclones. *Nature*, *422*(6929), 279–283. https://doi.org/10.1038/nature01481

Price, J. F. (1981). Upper ocean response to a hurricane. *Journal of Physical Oceanography*, *11*(2), 153–175. https://doi.org/10.1175/1520-0485(1981)011<0153:Uortah>2.0.Co;2

Price, J. F., Sanford, T. B., & Forristall, G. Z. (1994). Forced stage response to a moving Hurricane. *Journal of Physical Oceanography*, *24*(2), 233–260. https://doi.org/10.1175/1520-0485(1994)024<0233:Fsrtam>2.0.Co;2

Rienecker, M. M., Suarez, M. J., Gelaro, R., Todling, R., Bacmeister, J., Liu, E., et al. (2011). MERRA: NASA's Modern-Era Retrospective analysis for research and applications. *Journal of Climate*, *24*(14), 3624–3648. https://doi.org/10.1175/JCLI-D-11-00015.1

Rimac, A., Storch, J., Eden, C., & Haak, H. (2013). The influence of high-resolution wind stress field on the power input to near-inertial motions in the ocean: The influence of high-resolution winds. *Geophysical Research Letters*, *40*(18), 4882–4886. https://doi.org/10.1002/grl.50929

Shay, L. K., & Jacob, S. D. (2006). Relationship between oceanic energy fluxes and surface winds during tropical cyclone passage. In W. Perrie (Ed.), *Atmosphere-Ocean interactions II: Advances in fluid mechanics* (pp. 115–142). WIT Press.

Sun, B., Wang, S., Yuan, M., Wang, H., Jing, Z., Chen, Z., & Wu, L. (2021). Energy flux into near-inertial internal waves below the surface boundary layer in the global ocean. *Journal of Physical Oceanography*, *51*(7), 2315–2328. https://doi.org/10.1175/jpo-d-20-0276.1

Vincent, E. M., Lengaigne, M., Madec, G., Vialard, J., Samson, G., Jourdain, N. C., et al. (2012). Processes setting the characteristics of sea surface cooling induced by tropical cyclones. *Journal of Geophysical Research*, *117*(C2), C02020. https://doi.org/10.1029/2011jc007396

von Storch, J. S., & Lüschow, V. (2023). Wind power input to ocean near near-inertial waves diagnosed from a 5-km global coupled atmosphere-ocean general circulation model. *Journal of Geophysical Research: Oceans*, *128*(2), e2022JC019111. https://doi.org/10.1029/2022jc019111

Wang, G., Wu, L., Mei, W., & Xie, S. P. (2022). Ocean currents show global intensification of weak tropical cyclones. *Nature*, *611*(7936), 496–500. https://doi.org/10.1038/s41586-022-05326-4

Watanabe, M., & Hibiya, T. (2002). Global estimates of the wind-induced energy flux to inertial motions in the surface mixed layer. *Geophysical Research Letters*, *29*(8), 1239. https://doi.org/10.1029/2001GL014422

Whalen, C. B., de Lavergne, C., Naveira Garabato, A. C., Klymak, J. M., MacKinnon, J. A., & Sheen, K. L. (2020). Internal wave-driven mixing: Governing processes and consequences for climate. *Nature Reviews Earth & Environment*, *1*(11), 606–621. https://doi.org/10.1038/s43017-020-0097-z

Willoughby, H. E., Darling, R. W. R., & Rahn, M. E. (2006). Parametric representation of the primary hurricane vortex. Part II: A new family of sectionally continuous profiles. *Monthly Weather Review*, *134*(4), 1102–1120. https://doi.org/10.1175/mwr3106.1

Yang, B., & Hou, Y. (2014). Near-inertial waves in the wake of 2011 typhoon Nesat in the northern South China Sea. *Acta Oceanologica Sinica*, *33*(11), 102–111. https://doi.org/10.1007/s13131-014-0559-6

Zhang, H., Liu, X., Wu, R., Chen, D., Zhang, W., Shang, X., et al. (2020). Sea surface current response patterns to tropical cyclones. *Journal of Marine Systems*, *208*, 103345. https://doi.org/10.1016/j.jmarsys.2020.103345

References From the Supporting Information

Park, J. J., Kim, K., & Schmitt, R. W. (2009). Global distribution of the decay timescale of mixed layer inertial motions observed by satellite-tracked drifters. *Journal of Geophysical Research*, *114*(C11), C11010. https://doi.org/10.1029/2008jc005216

Supporting Information for

Tropical cyclones related wind power on oceanic near-inertial oscillations

Sheng Lin[1], Yuntao Wang[1*], Wen-Zhou Zhang[2,1*], Qin-Biao Ni[3], Fei Chai[2,1]

[1] State Key Laboratory of Satellite Ocean Environment Dynamics, Second Institute of Oceanography, Ministry of Natural Resources, Hangzhou 310012, China.

[2] State Key Laboratory of Marine Environmental Science, College of Ocean and Earth Sciences, Xiamen University, Xiamen 361102, China.

[3] Southern Marine Science and Engineering Guangdong Laboratory (Zhuhai), Zhuhai 519082, China.

Contents of this file

Introduction

The Supporting Information provides supplementary details regarding the selection of the threshold for identifying the drifters influenced by tropical cyclones (TCs) (Text S1). This information likely elaborates on the specific criteria or parameters used to determine the inclusion of drifters in the analysis.

Furthermore, to assess the reliability of the ERA5*1.22 adjustment method, two additional adjustments were performed based on the idealized vortex spatial structure proposed by Holland et al. (1980) and Willoughby et al. (2006) (Text S2). These adjustments aimed to compare and evaluate the performance of different adjustment methods in estimating the additional contribution of TCs to wind power on near-inertial oscillations (NIOs). The results of these adjustments, including the additional contribution of TCs to wind power on NIOs based on different wind fields, are presented in Table S1 and Figure S1. The findings from these additional adjustments are discussed in Text S2.

Text S1.

It is important to use spatial and temporal criteria that encompass the actual influential area of TCs where a threshold is defined to classify the drifters. Regardless of the chosen value, there will always be a division of drifters without the influence of TCs into those under the influence of TCs (or vice versa). Consequently, it is crucial to evaluate the impact of the selected threshold on accurately identifying the drifters influenced by TCs. In this study, the selected threshold is optimized based on the equations S1 (same as equation 3 in the manuscript) and equations S2 & S3. The total wind power on oceanic NIOs in each grid can be estimated as equations S1:

$$W_{total} = W_{tc} * P_{tc} + W_{climat} * (1 - P_{tc})$$

$$= \overbrace{(W_{tc} - W_{climat}) * P_{tc}}^{W_{contc}} + W_{climat} \quad (S1)$$

where $W_{tc} * P_{tc}$ is the contribution of TCs, $W_{climat} * (1 - P_{tc})$ is the contribution of climatology, and $(W_{tc} - W_{climat}) * P_{tc}$ is the additional contribution of TCs (W_{contc}), representing the value of underestimate when TCs are overlooked ($W_{total} - W_{climat}$).

When we divided the drifters without the influence of TCs into drifters under the influence of TCs, the wind power induced by TCs (W_{tc}) and the proportion of drifters under the influence of TCs (P_{tc}) in equation S1 change simultaneously. Giving a larger

2

proportion of drifters (P_{tc}') to the group under the influence of TCs, which contains the all of drifters under the influence of TCs (P_{tc}) and the parts of drifters without the influence of TCs ($P_{tc}' - P_{tc}$), the TC-related wind power (W_{tc}') becomes:

$$W_{tc}' = [W_{tc} * P_{tc} + W_{climat} * (P_{tc}' - P_{tc})] / P_{tc}' \quad (S2)$$

The total wind power on oceanic NIOs becomes:

$$W_{total}' = \overbrace{(W_{tc}' - W_{climat}) * P_{tc}'}^{W_{contc}'} + W_{climat}$$

$$= \overbrace{(W_{tc} - W_{climat}) * P_{tc}}^{W_{contc}'} + W_{climat} \quad (S3)$$

Please note that in equation S1, when comparing the values of W_{contc} and W_{total}, the value of W_{contc}' and W_{total}' in equation S3 do not change if P_{tc}' is larger than P_{tc}. This implies that the additional contribution of TCs (W_{contc}) is independent of P_{tc} and can largely mitigate errors caused by the threshold for drifter classification. Conversely, when drifters under the influence of TCs are mistakenly classified as drifters without TC influence (P_{tc}' less than P_{tc}), the impact of TCs (W_{contc}') will be underestimated.

Park et al. (2009) suggests that the majority of observed NIOs obviously decay within a week, which is especially true in the North Pacific between 15°N and 30°N that is less than 5 days. Meanwhile, Chen et al. (2013) found that the majority of NIOs induced by TCs had a decay timescale between 7 and 10 days. Although the majority of decay timescales of NIOs induced by TCs are less than 10 days, Chen et al. (2013) also found a near-inertial oscillation event with the longest e-folding timescale of 13.5 day. On the other hand, Lob et al. (2021) estimated the wind power on NIOs induced by a single TC using 19 days. As the timescale of TC-induced NIOs could vary for each individual TC, the deviation is unavoidable when we select a time threshold to assess whether the drifters are affected by TCs or not. To make sure the temporal criteria is equal or larger than actual influential time, we treat drifters with sampling times within the range of 3 days before the passage of typhoons to 20 days after typhoons as being influenced by the TCs, which is large enough as the majority of decay timescales of NIOs induced by TCs are less than 10 days.

Furthermore, the impact of the selected time threshold for identifying the drifters under the influence of TCs was evaluated. To assess the sensitivity of the TC-induced NIOs to the selected time range, an alternative range from -3 to 10 days was tested. The analysis revealed that the changes in TC-induced NIOs resulting from this alternative time range were minimal, amounting to less than 2% difference. This suggests that the chosen time threshold appears to be appropriate for capturing the influence of TCs on NIOs and subsequently estimating wind power accurately.

Text S2

To test the reliability of the ERA5*1.22 adjustment method, another two adjustments were conducted based on the idealized vortex spatial structure proposed by Holland et al. (1980) and Willoughby et al. (2006). These adjustments were conducted following the methodology outlined in Vincent et al. (2012). Before adding the idealized TC wind signal to the ERA5 wind fields, a filtering process was applied to remove the weak TC signal present in the ERA5 data. This was achieved by applying an 11-day running mean within 600 km around each cyclone track position, and with a linear transition from filtered to unfiltered winds between 600 and 1200 km. This filtering step helped prevent the overestimation of TC intensity by adding the idealized TC wind signal to the existing weak TC signal in the ERA5 data.

The estimated wind power values obtained using Holland and Willoughby adjustment methods are 0.054 TW and 0.053 TW, respectively (Table S1). These estimated wind power values account for 15% of the quasi-global integral (60°S to 60°N) of W_{total}. The fact that the values derived from different adjustment methods are comparable, indicating that the methods used are reliable.

Furthermore, the actual influencing time T_{tc} adjustments is also conducted based on the wind fields from Holland and Willoughby adjustment methods, i.e., TCs (T_{tc}) in Table S1. Figure S1a illustrates the meridional distribution of the zonally integrated wind power based on different wind fields. Notably, all maximum values of TC-related wind power on NIOs, derived from different wind field, occur at 17°N. These values range from 0.0014 TW (CCMP) to 0.0043 TW (Holland) (Figure S1a), surpassing the climatology wind power on NIOs at 17°N, which is 0.0008 TW. Consequently, TCs contribute at least 55% (CCMP) of the zonal integrated wind power (Figure 4c). The maximum value obtained using the three improved wind fields are 0.0032 TW (80%), 0.0038 TW (84%) and 0.0043 TW (86%), respectively. These values are comparable to the maximum value of 0.038 TW in the Northern Hemisphere when not considering the influence of TCs (Figure 4a). Based on the three improved wind fields, TCs could contribute more than 15% of the global wind power on NIOs, which is larger than that from CCMP (6%) and ERA5 (10%).
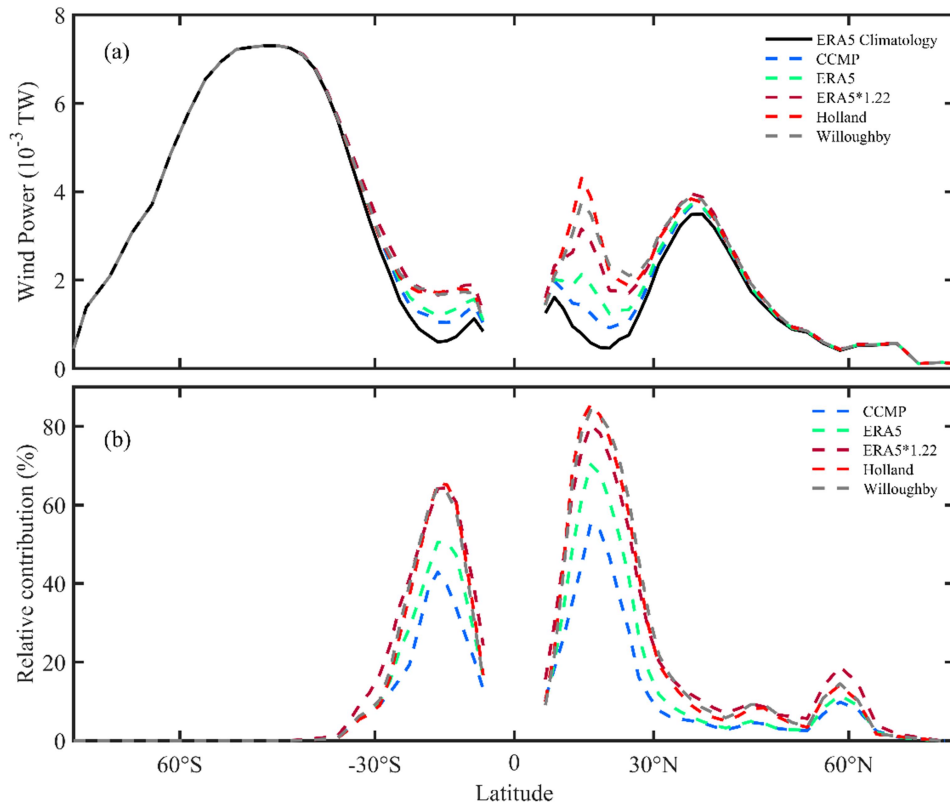
Figure S1 (**a**) Meridional distribution of zonally integrated wind power on NIOs based on different wind fields. (**b**) Percentage of TC-related wind power on oceanic NIOs (W_{contc}/W_{total}) based on different wind fields.

Table S1. The quasi-global integral climatology and TCs related wind power on NIOs based on different wind fields (TW). Percent in brackets are the relative contribution of TCs to W_{total}. ERA5 *1.22, Holland and Willoughby are adjusting wind fields during TCs based on the mean difference, holland et al. (1980) and Willoughby et al. (2006) idealized vortex spatial structure.

Wind fields	CCMP	ERA5	ERA5	ERA5	ERA5
TCs adjustment	-	-	ERA5 *1.22	Holland	Willoughby
Climatology	0.33	0.31	0.31	0.31	0.31
TCs (P_{tc})	0.018 (5%)	0.028 (8%)	0.051 (14%)	0.054 (15%)	0.053 (15%)
TCs (T_{tc})	0.023 (6%)	0.034 (10%)	0.061 (16%)	0.065 (17%)	0.064 (17%)

Reference

Chen, G., Xue, H., Wang, D., Xie, Q. (2013). Observed near-inertial kinetic energy in the northwestern South China Sea. *Journal of Geophysical Research: Oceans,* *118*(10), 4965–4977.

129 Holland, G. J. (1980). An Analytic Model of the Wind and Pressure Profiles in
130   Hurricanes. *Monthly Weather Review, 108*(8), 1212–1218.
131 Lob, J., Kohler, J., Walter, M., Mertens, C., Rhein, M. (2021). Time series of near-inertial
132   gravity wave energy fluxes: The effect of a strong wind event. *Journal of
133   Geophysical Research-Oceans, 126*(10), e2021JC017472.
134 Park, J. J., Kim, K., Schmitt, R. W. (2009). Global distribution of the decay timescale of
135   mixed layer inertial motions observed by satellite-tracked drifters. *Journal of
136   Geophysical Research-Oceans*, *114*, C11010.
137 Vincent, E. M., Lengaigne, M., Madec, G., Vialard, J., Samson, G., Jourdain, N. C., et al.
138   (2012). Processes setting the characteristics of sea surface cooling induced by
139   tropical cyclones. Journal of Geophysical Research, 117, C02020.
140 Willoughby, H. E., Darling, R. W. R., Rahn, M. E. (2006). Parametric representation of
141   the primary hurricane vortex. part II: a new family of sectionally continuous
142   profiles. *Monthly Weather Review, 134*(4), 1102–1120.